POLITECNICO DI TORINO
Repository ISTITUZIONALE

Impact of Predictive Battery Thermal Management for a 48V Hybrid Electric Vehicle

(Article begins on next page)

18 September 2024

Impact of Predictive Battery Thermal Management for a 48V Hybrid Electric Vehicle

Pier Giuseppe Anselma*,†, Federico Miretti*,‡, Ezio Spessa*,‡
*CARS@PoliTo - Center for Automotive Research and Sustainable Mobility,
Politecnico di Torino, C.so Ferrucci 112, Torino, TO 10138, Italy
†Department of Mechanical and Aerospace Engineering (DIMEAS)
Politecnico di Torino, Corso Duca degli Abruzzi 24, Torino, TO 10129, Italy
‡Department of Energy "Galileo Ferraris" (DENERG)
Politecnico di Torino, Corso Duca degli Abruzzi 24, Torino, TO 10129, Italy
Email: federico.miretti@polito.it

Abstract—Overheating of battery packs in electrified vehicles is detrimental to their lifetime and performance. Unfortunately, designing a control strategy that ensures battery protection without jeopardizing fuel economy is not a straightforward task. In this paper, we investigate battery temperature-sensitive optimal energy management for a 48V mild-hybrid electric vehicle to prevent overheating with minimal fuel consumption increase. Indeed, this family of hybrid architectures is challenging due to the absence of an active cooling system.

In particular, we modeled a p0 parallel-hybrid with a 48V battery pack and we employed dynamic programming to numerically investigate the fuel economy capability while tracking the battery pack temperature.

First, we tuned a battery current-constrained powertrain control strategy in order to avoid battery overheating, which could be easily implemented on-board. Then, we implemented a predictive temperature-constrained strategy that exploits the a priori knowledge of driving conditions and temperature constraints to maximize fuel economy.

Results show that both strategies are able to meet the battery temperature constraints, although the predictive temperature-constrained control strategy outperforms the current-constrained strategy in terms of fuel economy. This case study demonstrates the theoretical benefits of a predictive battery thermal management for 48V mild hybrids.

Index Terms—mild hybrid, hybrid electric, predictive, thermal management, passive cooling, battery

I. Introduction

Mild hybrid electric vehicles (HEVs) embedding a 48 volt battery pack are currently emerging as a viable and cost-effective technology to reduce fuel consumption and tailpipe emissions [1]. Energy management strategies (EMSs) need to be developed for optimally controlling the power split between internal combustion engine and belt-starter generator (BSG) of 48V HEVs. To this end, different EMS approaches have been developed over the years, including for example rule-based [2], Pontryagin's Minimum Principle [3], and reinforcement learning [4].

The 48 volt battery pack is a key component in mild HEVs. Nevertheless, the above mentioned research works consider important assumptions concerning modeling and management of the 48V battery pack. For example, the evolution of the 48V battery pack temperature over time is not modeled neither in [3] nor in [4]. Alternatively, the maximum charge and discharge current are set to be heuristically limited by the HEV EMS in order to prevent overheating the 48V battery pack in [2].

Temperature is a key aspect in li-ion battery pack of electrified vehicles. One major related challenge is to limit it to prevent thermal runaway and accelerated aging [5] [6] while not penalizing energy economy due to the auxiliary power dissipated by the cooling system [7]. Recent research works attempted to investigate the optimal trade-off between these issues.

For example, in 2014 Johri et al. implemented a battery temperature-aware dynamic programming (DP) formulation to determine the optimal battery cooling requirements of a power-split full HEV [8]. Moreover, predictive battery thermal management systems for full and plug-in HEVs have been proposed that exploit either the prediction of future vehicle operating conditions [9] or real-time traffic and road information [10].

The previously mentioned literature however mainly focuses on active cooling of battery packs for full and plug-in HEVs, while little research has been published concerning 48V HEVs, which are peculiar in that they usually do not use a dedicated cooling circuit. Rather, they use a passive cooling system, which means that the EMS ensures compliance with battery thermal limits by appropriately limiting its maximum charge and discharge currents.

Nevertheless, predictive battery pack thermal management could potentially lead to significant fuel savings for commercially available 48V HEV powertrains as well. To answer this research gap, this paper describes a temperature-aware optimal control framework for 48V HEV powertrains that takes into account battery thermal limits.

Two main achievements can be accomplished in this way. First, this papers presents an assessment of the theoretical fuel saving achievable by a 48V HEV by implementing predictive battery pack thermal management systems, thus making the case for technological viability of these systems. Second, the off-line methdology described in this paper for optimizing 48V HEV powertrain operation lays the foundations for developing

and benchmarking real-time capable 48V battery pack predictive thermal management systems.

The rest of this paper is organized as follows:

II. SIMULATION MODEL

In order to estimate the fuel consumption while tracking the battery's temperature, we adopted a powertrain model which evaluates the required torque as a function of a given vehicle driving mission, which is a vehicle speed profile. This type of simulation models is known as a *backward-facing* [11], [12] or *quasi-static* model [13] and it is commonly used in conjunction with an EMS optimization algorithm such as Dynamic Programming in order to assess fuel economy and perform other energy analyses of hybrid electric powertrains [14].
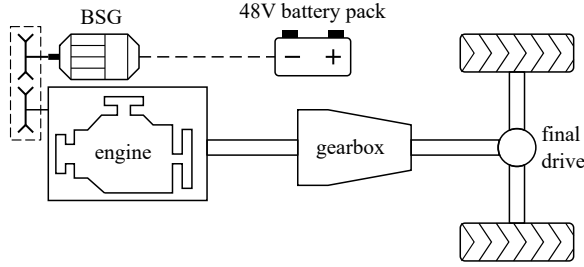

Fig. 1. p0 HEV architecture.

A tractive effort was evaluated with a longitudinal vehicle model in order to match the speed profile prescribed by the driving mission and then propagated through the drivetrain to obtain a torque request. This torque request was then split at the torque-coupling device into an engine and e-machine torque which were used to evaluate fuel consumption, which constitutes the running cost in the EMS objective function (7), and battery power, which is an input to the electrical and thermal battery models.

First, the total vehicle resistance force was evaluated as a function of the vehicle speed v_{veh} using a set of coast-down coefficients [15], [16]. Then, the required tractive effort, equal to the sum of the resistance force and the vehicle equivalent inertia, is translated into a torque request to the thermal engine and the e-machine via a torque-split coefficient α:

$$\alpha = \frac{T_{\text{em,gb}}}{T_{\text{req}}}, \tag{1}$$

where $T_{\text{em,gb}}$ is the e-machine's torque contribution at the gearbox input and T_{req} is the required torque at the gearbox input.

The engine fuel rate $\dot{m}_{\text{f}}$ was then evaluated using a steady-state map as a function of its speed ω_{eng} and torque T_{eng} [16]–[18]:

$$\dot{m}_{\text{f}} = \dot{m}_{\text{f}} \left(\omega_{\text{eng}}, T_{\text{eng}} \right); \tag{2}$$

and the electrical power drawn from or provided to the battery P_{b} was evaluated using a loss map $P_{\text{em,loss}}$ characterizing the e-machine and inverter losses as a function of its speed ω_{em} and torque T_{em}

$$P_{\text{b}} = \omega_{\text{em}} T_{\text{em}} + P_{\text{em,loss}} \left(\omega_{\text{em}}, T_{\text{em}} \right). \tag{3}$$

The battery's SOC dynamics was modeled using a simple internal resistance model:

$$\dot{\sigma} = \frac{i_{\text{b}}}{Q_{\text{b}}}, \tag{4}$$

$$i_{\text{b}} = \frac{v_{\text{oc}} - \sqrt{v_{\text{oc}}^2 - 4R_{\text{eq}}P_{\text{b}}}}{2R_{\text{eq}}}, \tag{5}$$

where i_{b}, v_{oc}, R_{eq} and Q_b are the battery current, open-circuit voltage, equivalent resistance and capacity. The open-circuit voltage and equivalent resistance were characterized as a function of SOC and temperature of the battery.

The battery's thermal dynamics were modeled by assuming that the most relevant contributions are the heat generated by Joule effect and the heat transferred to the surrounding environment by convection [19]–[21]. This convective heat transfer is proportional to the temperature difference between the battery (T_{b}) and the surrounding air (T_{env}) via the heat exchange area A_{b} and a heat transfer coefficient h.

The temporal evolution of the battery temperature was then obtained from the following energy balance:

$$\dot{T}_{\text{b}} = \frac{1}{C_{\text{b}}} \left(R_{\text{eq}} i_{\text{b}}^2 - h A_{\text{b}}(T_{\text{b}} - T_{\text{env}}) \right), \tag{6}$$

where C_{b} is the battery's thermal capacity.

III. ENERGY MANAGEMENT STRATEGY

The HEV powertrain architecture under consideration was simulated being controleld by a charge-sustaining fuel-optimal EMS using a DP algorithm. In particular, the described HEV numerical model was fed to a dedicated optimal control tool called DynaProg[1] [22].

The SOC and temperature of the battery were identified as the state variables while the torque-split coefficient (1) and the gear number were set as control variables to be controlled in order to minimize the cost functional:

$$J(\sigma_0, T_{\text{b},0}) = \int_{t_0}^{t_{\text{f}}} \dot{m}_{\text{f}} \left(\omega_{\text{eng}}, T_{\text{eng}} \right) \, \text{d}t, \tag{7}$$

where σ_0 and $T_{\text{b},0}$ are the initial SOC and battery temperature.

Charge-sustaining operation was achieved by constraining the battery SOC at the end of the driving mission to be equal to the starting SOC, which was set to 0.6.

In addition to the charge-sustaining constraint, other constraints were set on the powertrain components in order not to exceed their physical capabilities, such as the engine and e-machine maximum speed and torque. The battery's SOC was also set not to exceed lower and upper thresholds of 0.4 and 0.8 respectively.

To assess the potential effect of a thermal-aware optimal control strategy, we set up and simulated three test cases for the same powertrain, whose characteristics are reported in Table I, using three different control strategies, a temperature-unaware strategy, a battery current-constrained strategy and temperature-constrained strategy.

[1]Source code is available at https://github.com/fmiretti/DynaProg, toolbox package available at https://www.mathworks.com/matlabcentral/fileexchange/84260-dynaprog.

TABLE I
MAIN VEHICLE DATA.

Component	Parameter	Value
Vehicle	Mass	1978 kg
	First coast-down coefficient	198 N
	Second coast-down coefficient	0.927 N/(ms)
	Third coast-down coefficient	0.423 N/(ms)^2
	Tyre radius	0.329 m
Engine	Configuration	inline-four cylinders
	Displacement	2.0 l
	Rated power	243 kW
	Maximum torque	450 Nm
E-machine	Type	IPMSM
	Rated power	30 kW
	Maximum torque	150 Nm
Battery	Type	Li-ion 14s11p
	Nominal capacity	25 Ah
	Nominal voltage	48 V
	Heat capacity	7.12 kJ/kgK
	Heat transfer coefficient	5 W/(m^{2}K)

Vehicle chassis data, including the mass, tire radius, and road load coefficients, relate to the Maserati Ghibli Hybrid model year 2021 and they were obtained from the US Environmental Protection Agency (EPA) database [23]. Operational maps for the engine and BSG were generated using the respective tools implemented in Amesim software [24], [25]. Electrical and thermal parameters of the 48V battery pack were taken from [26].

The temperature-unaware strategy does not attempt to keep the battery temperature under control in any way. The remaining two strategies aim to keep the battery's temperature below 40 °C; but they differ from each other in that for the temperature-constrained strategy we directly set a constraint on this temperature, while for the current-constrained strategy we se a constraint on the maximum battery current and tuned it to meet the same temperature constraint.

Because of the high performance and the high potential for recuperation through regenerative braking enabled by the hybrid architecture under study, we expected the temperature-unaware strategy to produce an excessive amount of Joule heating which in turn would lead the battery temperature to dangerously high levels. In addition, because the temperature-unaware strategy is less constrained, we expected the fuel consumption of the other two strategies to be slightly higher.

These expectations were verified by the simulation results, as discussed in Section IV.

IV. RESULTS AND DISCUSSION

The strategies were compared by simulating the hybrid powertrain on the Worldwide Light Vehicle Test Procedure (WLTP) driving mission, with an initial SOC of 0.6 and an initial battery temperature equal to the environment temperature. The environment temperature, which influences the heat

[2]Maximum and mean currents are evaluated from the current profiles in absolute value.

exchanged by with the battery through (6), was set to 10° C, 20° C and 30° C, respectively.

As illustrated by Figures 2, 3 and 4, the temperature-unaware strategy takes full advantage of its electric components to reduce fuel consumption as much as possible, producing higher currents in the process and therefore heating up the battery up to significantly more than 40 °C.

The temperature-aware[3] strategy, on the other hand, significantly shaves off all current peaks in order to keep the battery temperature below 40 °C.

For example, let us consider the case for an environment temperature of 20 °C, illustrated in Figure 3. As expected, the temperature-unaware strategy produced the lowest fuel consumption at 6.20 l/(100 km), against the temperature-constrained strategy's 6.36 l/(100 km); though the extent of this gap is a result worth discussing. Notably, setting a constraint on the battery temperature influenced fuel consumption by 2.6 %, which is a remarkable increase; a possible explanation lies in the characteristics of the hybrid powertrain under study. Turning our attention to the current-constrained strategy, we found that setting a limit current of 130 A produced a maximum temperature of 39.6 °C, comparable to that achieved by the temperature-constrained strategy, with an increased fuel consumption at 6.36 l/(100 km).
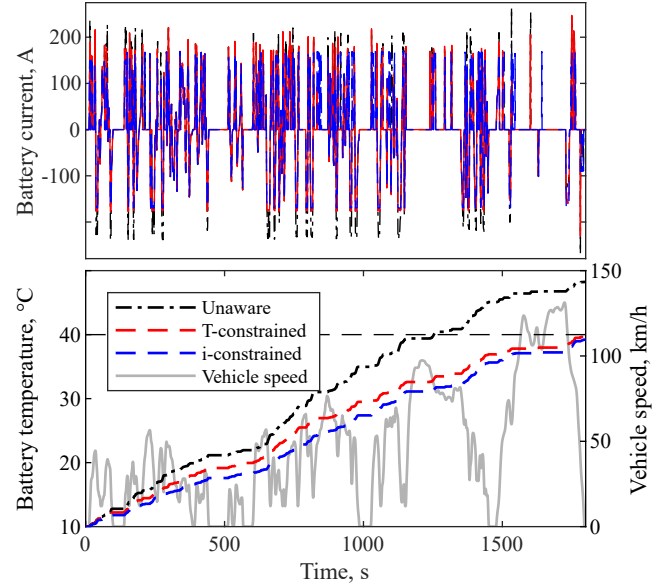

Fig. 2. Simulated battery current and temperature profiles, for an environment temperature of 10 °C.

Statistics for the DP results in WLTP considering both the temperature-aware strategy (*T-constrained*) and the current constrained strategy (*i-constrained*) for values of environment temperature equal to 10° C, 20° C and 30° C are reported in Table II. The EM loss and average efficiency have been calculated by interpolating in the corresponding two-dimensional lookup table with torque and speed as independent variables.

[3]Note that we use the terms *temperature-aware* and *temperature-constrained* interchangeably throughout this text.

|	10 °C		20 °C		30 °C	
	T-constrained	i-constrained	T-constrained	i-constrained	T-constrained	i-constrained
EM loss, MJ	5.50	5.30	5.28	5.27	5.72	5.27
Average EM efficiency	0.737	0.734	0.715	0.708	0.670	0.655
Belt loss, kJ	96.6	96.9	92.2	99.2	83.1	95.3
Battery loss, kJ	211	208	139	147.8	71.2	89.0
Battery current constraint, A	-	170	-	130	-	90
Max battery current^2, A	247	170	190	130	247	90.0
Mean battery current^2, A	44.6	45.1	36.7	39.1	24.5	31.6
Engine mech. energy, MJ	16.3	16.3	16.5	16.5	16.8	16.7
Average engine efficiency, kJ	0.327	0.321	0.325	0.312	0.322	0.310
Fuel economy, l/100km	6.27	6.30	6.36	6.43	6.51	6.79
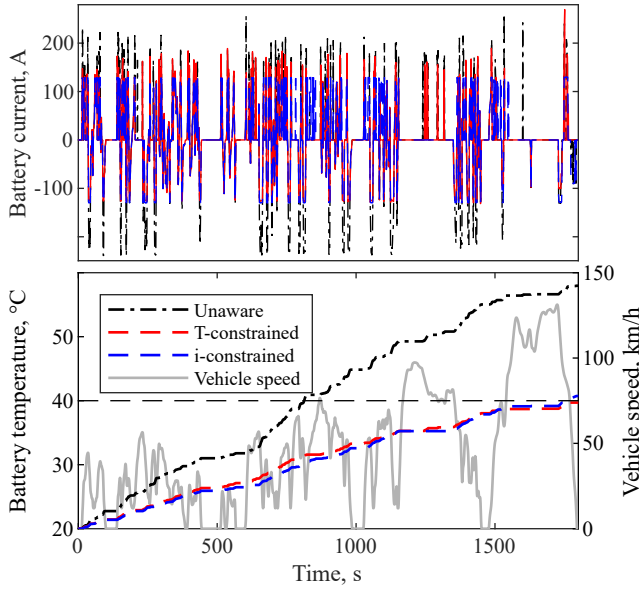
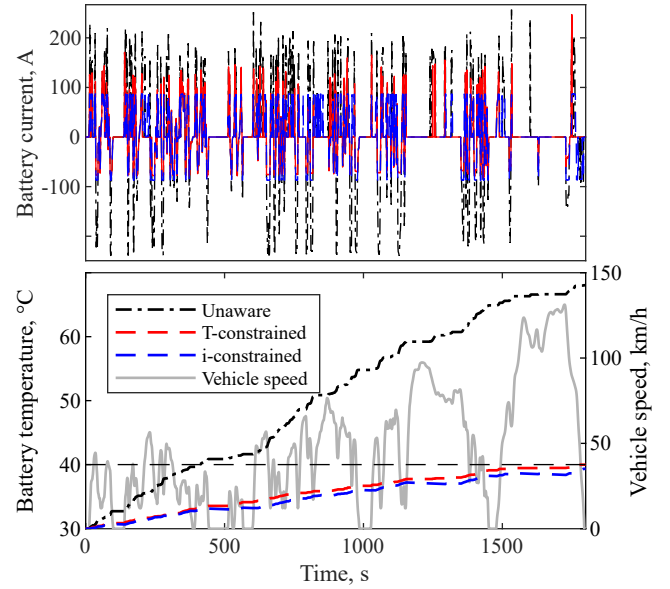Fig. 3. Simulated battery current and temperature profiles, for an environment temperature of 20 °C.

Fig. 4. Simulated battery current and temperature profiles, for an environment temperature of 30 °C.

In general, 0.5 % to 4.3 % fuel economy improvement can be achieved by the temperature-aware strategy compared with the current-aware strategy for environment temperatures equal to 10° C and 30° C, respectively. Different contributions can be identified for the fuel economy enhancement predicted by the proposed temperature-aware strategy, including:
1) shifting the operating points of both the EM and the engine towards higher efficiency areas,
2) reducing the mechanical loss of the belt in the BSG.

The numerical experiments hint that the potential for fuel economy improvement thanks to the proposed temperature-aware strategy proportionally increases with the value of the environment temperature. Indeed, looking at Table II, the value of maximum battery current that the current-constrained strategy is allowed to operate while complying with the 40° C temperature limit markedly decreases for high environment temperatures. This in turn poses quite limiting constraints

on the operation of the entire electrified powertrain. For example, the EM is forced to operate in low-efficient low-torque regions, which results in 13 % only average efficiency when the environment temperature is 30° C. On the other hand, the proposed temperature-aware strategy exploits the a priori information of the drive cycle and the embedded battery thermal model to keep exploiting the BSG and 48V battery pack operation and minimize the fuel consumption increase at high values of environment temperatures.

When it comes to the battery pack itself, the current-constrained strategy does not seem to make the best use of it at high values of environment temperatures, as reflected in the lower loss in Table II compared with the temperature-constrained strategy when the environment temperature is equal to 30° C. On the other hand, the temperature-aware strategy increases the use of the battery pack to improve the performance of the remaining components of the electrified

powertrain, as suggested by the lower EM loss, the higher EM efficiency and the higher engine efficiency in Table II.

Another interesting result is that the temperature-constrained strategy produces higher peak currents, but lower mean currents. This reflects its ability to use the battery at the best time given the EMS target of minimizing fuel consumption; while a direct constraint on the battery current reduces the flexibility with which the EMS optimization algorithm can pursue the same target.

Overall, these results corroborate the effectiveness of the proposed temperature-aware strategy in terms of electrified powertrain efficiency improvement and fuel economy enhancement, especially for high values of environment temperature.

In general, the high performance of the e-machine enables great fuel savings because of its high recuperation capability as well as a remarkable ability to power the vehicle in all acceleration phases. However, since the battery voltage is limited to 48 V, fully exploiting this capabilities inevitably produces high currents. The temperature-constrained strategy, indirectly limiting the maximum current, reduces the extent to which the electrical part can be used to achieve the maximum fuel saving.

V. Conclusions

The simulation case studies presented here show how smart control strategies can effectively take advantage of knowledge of anticipated future driving conditions in order to prevent battery overheating while keeping fuel consumption increase at a minimum[4]. Moreover, the obtained results suggest that setting a constraint on the battery current, when compared to a direct constraint on the battery temperature, can be equally effective in preventing overheating although it is slightly outperformed in terms of fuel economy.

Numerical experiments conducted with different ambient temperatures show that the advantages of a temperature-aware control strategy grow larger as the environment temperature increases.

One major limitation of this work is that we did not consider different driving scenarios. The experiments where conducted by driving the vehicle through the WLTP cycle, corresponding to a traveled distance of approximately 22 km composed by a mix of urban, suburban and highway driving scenarios. The proposed strategy was only tested for a short traveled distance (compared to the relatively slow thermal dynamics of a battery pack) which averages out a variety of scenarios; an obvious extension of this work would be to assess its performance with longer traveled distances and selective driving scenarios.

Secondly, it should be noted that the deterministic dynamic programming algorithm that was used in this work to obtain fuel-optimal control strategies assumes perfect knowledge of future driving conditions. Hence, the fuel economy that we evaluated in our experiments should be interpreted as an upper limit that could theoretically be achieved. An important future step is therefore to test a variety of prediction algorithms

for future driving conditions with different levels of data availability, in order to assess to what extent can a real-time EMS fulfill this performance.

References

[1] Z. Liu, A. Ivanco, and Z. S. Filipi, "Impacts of real-world driving and driver aggressiveness on fuel consumption of 48v mild hybrid vehicle," *SAE International Journal of Alternative Powertrains*, vol. 5, no. 2, pp. 249–258, apr 2016.

[2] R. M. Bagwe, A. Byerly, E. C. dos Santos, and Ben-Miled, "Adaptive rule-based energy management strategy for a parallel HEV," *Energies*, vol. 12, no. 23, p. 4472, nov 2019.

[3] L. Thibault, A. Sciarretta, and P. Degeilh, "Reduction of pollutant emissions of diesel mild hybrid vehicles with an innovative energy management strategy," in *2017 IEEE Intelligent Vehicles Symposium (IV)*. IEEE, jun 2017.

[4] B. Xu, F. Malmir, D. Rathod, and Z. Filipi, "Real-time reinforcement learning optimized energy management for a 48v mild hybrid electric vehicle," in *SAE Technical Paper Series*. SAE International, apr 2019.

[5] C. Yu, G. Ji, C. Zhang, J. Abbott, M. Xu, P. Ramaekers, and J. Lu, "Cost-efficient thermal management for a 48v li-ion battery in a mild hybrid electric vehicle," *Automotive Innovation*, vol. 1, no. 4, pp. 320–330, nov 2018.

[6] P. G. Anselma, P. Kollmeyer, G. Belingardi, and A. Emadi, "Multi-objective hybrid electric vehicle control for maximizing fuel economy and battery lifetime," in *2020 IEEE Transportation Electrification Conference & Expo (ITEC)*. IEEE, jun 2020.

[7] P. G. Anselma, M. D. Prete, and G. Belingardi, "Battery high temperature sensitive optimization-based calibration of energy and thermal management for a parallel-through-the-road plug-in hybrid electric vehicle," *Applied Sciences*, vol. 11, no. 18, p. 8593, sep 2021.

[8] R. Johri, W. Liang, and R. McGee, "Hybrid electric vehicle energy management with battery thermal considerations using multi-rate dynamic programming," in *ASME 2013 Dynamic Systems and Control Conference*. American Society of Mechanical Engineers, oct 2013.

[9] M. R. Amini, H. Wang, X. Gong, D. Liao-McPherson, I. Kolmanovsky, and J. Sun, "Cabin and battery thermal management of connected and automated HEVs for improved energy efficiency using hierarchical model predictive control," *IEEE Transactions on Control Systems Technology*, vol. 28, no. 5, pp. 1711–1726, sep 2020.

[10] C. Zhu, F. Lu, H. Zhang, J. Sun, and C. C. Mi, "A real-time battery thermal management strategy for connected and automated hybrid electric vehicles (CAHEVs) based on iterative dynamic programming," *IEEE Transactions on Vehicular Technology*, vol. 67, no. 9, pp. 8077–8084, sep 2018.

[11] P. Pettersson, B. Jacobson, F. Bruzelius, P. Johannesson, and L. Fast, "Intrinsic differences between backward and forward vehicle simulation models," *IFAC-PapersOnLine*, vol. 53, no. 2, pp. 14 292–14 299, 2020.

[12] G. Mohan, F. Assadian, and S. Longo, "Comparative analysis of forward-facing models vs backward-facing models in powertrain component sizing," in *Hybrid and Electric Vehicles Conference 2013 (HEVC 2013)*. Institution of Engineering and Technology, 2013.

[13] L. Guzzella and A. Amstutz, "CAE tools for quasi-static modeling and optimization of hybrid powertrains," *IEEE Transactions on Vehicular Technology*, vol. 48, no. 6, pp. 1762–1769, 1999.

[14] O. Sundström, L. Guzzella, and P. Soltic, "Optimal hybridization in two parallel hybrid electric vehicles using dynamic programming," *IFAC Proceedings Volumes*, vol. 41, no. 2, pp. 4642–4647, 2008.

[15] C. E. Chapin, "Road load measurement and dynamometer simulation using coastdown techniques," in *SAE Technical Paper Series*. SAE International, jun 1981.

[16] M. Ehsani, Y. Gao, S. E. Gay, and A. Emadi, *Modern Electric, Hybrid Electric, and Fuel Cell Vehicles*. CRC Press, dec 2004.

[17] J. D. Bishop, M. E. Stettler, N. Molden, and A. M. Boies, "Engine maps of fuel use and emissions from transient driving cycles," *Applied Energy*, vol. 183, pp. 202–217, dec 2016.

[18] J. Heywood, *Internal Combustion Engine Fundamentals*. McGraw-Hill Education Ltd, 2018.

[19] C. Forgez, D. V. Do, G. Friedrich, M. Morcrette, and C. Delacourt, "Thermal modeling of a cylindrical LiFePO4/graphite lithium-ion battery," *Journal of Power Sources*, vol. 195, no. 9, pp. 2961–2968, may 2010.

---

[4]We called this type of strategy *temperature-aware*.

[20] T. Huria, M. Ceraolo, J. Gazzarri, and R. Jackey, "High fidelity electrical model with thermal dependence for characterization and simulation of high power lithium battery cells," in *2012 IEEE International Electric Vehicle Conference*.   IEEE, mar 2012.

[21] L. Saw, Y. Ye, and A. Tay, "Electro-thermal characterization of lithium iron phosphate cell with equivalent circuit modeling," *Energy Conversion and Management*, vol. 87, pp. 367–377, nov 2014.

[22] F. Miretti, D. Misul, and E. Spessa, "DynaProg: Deterministic dynamic programming solver for finite horizon multi-stage decision problems," *SoftwareX*, vol. 14, p. 100690, jun 2021.

[23] US EPA (United States Environmental Protection Agency), "Data on cars used for testing fuel economy," *[online] https://www.epa.gov/compliance-and-fuel-economy-data/data-cars-used-testing-fuel-economy*, (accessed 9 Dec 2021).

[24] G. Alix, J.-C. Dabadie, and G. Font, "An ICE map generation tool applied to the evaluation of the impact of downsizing on hybrid vehicle consumption," in *SAE Technical Paper Series*.   SAE International, sep 2015.

[25] F. L. Berr, A. Abdelli, D.-M. Postariu, and R. Benlamine, "Design and optimization of future hybrid and electric propulsion systems: An advanced tool integrated in a complete workflow to study electric devices," *Oil & Gas Science and Technology – Revue d'IFP Energies nouvelles*, vol. 67, no. 4, pp. 547–562, jul 2012.

[26] S. Luciani, S. Feraco, A. Bonfitto, and A. Tonoli, "Hardware-in-the-loop assessment of a data-driven state of charge estimation method for lithium-ion batteries in hybrid vehicles," *Electronics*, vol. 10, no. 22, p. 2828, nov 2021.